ORGANIZATION OF THE ROSY LOCUS IN *DROSOPHILA MELANOGASTER*: FURTHER EVIDENCE IN SUPPORT OF A *CIS*-ACTING CONTROL ELEMENT ADJACENT TO THE XANTHINE DEHYDROGENASE STRUCTURAL ELEMENT[1]

M. McCARRON, J. O'DONNELL[2] AND A. CHOVNICK

Genetics and Cell Biology Section, Biological Sciences Group, The University of Connecticut, Storrs, Connecticut 06268

AND

B. S. BHULLAR, J. HEWITT AND E. P. M. CANDIDO

Department of Biochemistry, University of British Columbia, Vancouver, British Columbia V6T 1W5

Manuscript received July 14, 1978

ABSTRACT

The present report summarizes our recent progress in the genetic dissection of an elementary genetic unit in a higher organism, the rosy locus (*ry*:3–52.0) in *Drosophila melanogaster*. Pursuing the hypothesis that the rosy locus includes a noncoding control region, as well as a structural element coding for the xanthine dehydrogenase (XDH) peptide, experiments are described that characterize and map a rosy locus variant associated with much lower than normal levels of XDH activity. Experiments are described that fail to relate this phenotype to alteration in the structure of the XDH peptide, but clearly associate this character with variation in number of molecules of XDH per fly. Large-scale fine-structure recombination experiments locate the genetic basis for this variation in the number of molecules of XDH per fly to a site immediately to the left of the XDH structural element within a region previously designated as the XDH control element. Moreover, experiments clearly separate this "underproducer" variant site from a previously described "overproducer" site within the control region. Examination of enzyme activity in electrophoretic gels of appropriate heterozygous genotypes demonstrates the *cis*-acting nature of this variation in the number of molecules of XDH. A revision of the map of the rosy locus, structural and control elements is presented in light of the additional mapping data now available.

IN recent years, increasing attention has been directed to questions concerning the structure, function and regulation of elementary genetic units in higher organisms. Emerging from several experimental directions is the proposition that the eukaryotic gene is a much larger entity than its prokaryotic counterpart, and

[1] This investigation was supported by research grants, GM-09886 and GM-22753 from the Public Health Service, BMS74-19628 from the National Science Foundation, and a research grant from The Medical Research Council of Canada.

[2] Present address: Department of Biology, Carnegie-Mellon University, Pittsburgh, Pennsylvania 15213.

that the excess DNA is present in the form of noncoding sequences serving regulatory functions. Additionally, recent studies of several eukaryotic gene sequences have revealed that the structural information, in these cases, is not continuous, but rather is interrupted by noncoding segments that may or may not be removed in the production of mRNA (BRACK and TONEGAWA 1977; BREATHNACH, MANDEL and CHAMBON 1977; JEFFREYS and FLAVELL 1977; LAI *et al.* 1978; TILGHMAN *et al.* 1978a,b; MCREYNOLDS *et al.* 1978; WEINSTOCK *et al.* 1978). Indeed, a nontranscribed insert has also been identified in the 28S rDNA of *Drosophila melanogaster* (GLOVER and HOGNESS 1977; PELLEGRINI, MANNING and DAVIDSON 1977; WELLAUER and DAWID 1977; WHITE and HOGNESS 1977). These intriguing observations have already generated considerable speculation (BLAKE 1978; DOOLITTLE 1978; GILBERT 1978). The pursuit of these and other issues concerning the structure, function and regulation of genes in higher organisms will require specific genetic units whose DNA is marked and genetically mapped in order to permit identification and ordering of structural, regulatory and insertion sequences, and to relate these components to their specific functions. For some years, major emphasis in research of the Storrs laboratory has been directed towards the development of such an experimental system, utilizing the rosy locus in *Drosophila melanogaster* (*ry*:3–52.0).

Prior studies have shown that the rosy locus consists of a single structural element coding for a polypeptide of 150,000 daltons, which, as a homodimer, functions as the enzyme xanthine dehydrogenase (XDH) (GELBART *et al.* 1974; GELBART, MCCARRON and CHOVNICK 1976; EDWARDS, CANDIDO and CHOVNICK 1977). Moreover, evidence has been presented that argues for the existence of a *cis*-acting control element located adjacent to the left (centromere-proximal) side of the XDH structural element (CHOVNICK *et al.* 1976; EDWARDS, CANDIDO and CHOVNICK 1977).

This report presents additional genetic data, which, together with the prior observations, provide a compelling argument for the control element.

MATERIALS AND METHODS

The genetic system: Figure 1 presents a genetic map of the centromere-proximal region of chromosome 3, noting the rosy region and closely linked gene markers used in this investigation. Previous reports have described this experimental system, as well as our genetic and biochemical nomenclature (CHOVNICK *et al.* 1976; CHOVNICK, GELBART and MCCARRON 1977).

Rosy locus variants have been the subject of an intensive and continuing intragenic mapping analysis. Figure 2 summarizes our recent progress in this effort. Figure 2A presents a map of XDH$^-$, noncomplementing, rosy eye color mutant sites. Estimation of the boundaries of the XDH coding element is provided by the maps of three classes of unambiguous coding element site variants presented in Figure 2B (XDH$^-$, allele-complementing, rosy eye color mutant sites),

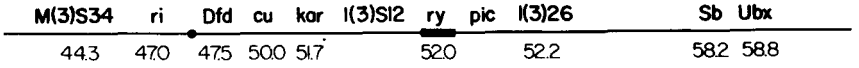

FIGURE 1.—A genetic map of the centromere proximal region of chromosome 3. Map positions of various mutants used in this investigation are indicated. Mutants not described in LINDSLEY and GRELL (1968) are discussed in CHOVNICK *et al.* (1976).

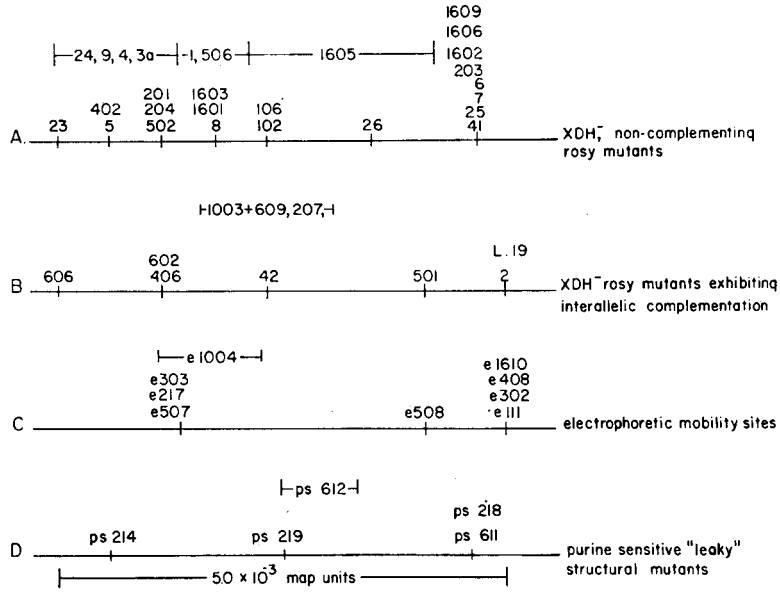

FIGURE 2.—Genetic fine-structure maps of rosy locus sites. Map locations of unambiguous structural element variants (B, C, and D) are positioned relative to map of XDH⁻ noncomplementing mutants (A).

Figure 2C (electrophoretic mobility sites) and Figure 2D (purine-sensitive "leaky" structural mutant sites). The left boundary is set by the leftmost allele-complementing site mutant, ry^{606}. On the basis of comparative recombination data and the failure of large-scale tests with ry^{606} to produce recombinants, the noncomplementing site mutant, ry^{23}, must also mark the left border. At the right end of the map, several electrophoretic sites and the complementing mutants, ry^{2} and $ry^{L.19}$, identify the right boundary of the coding element, with no known XDH variants beyond them. The maps of Figure 2 position 51 sites to the right of our present left boundary of the XDH structural element. In fact, an additional nine sites (not indicated) map in the structural element.

In addition to electrophoretic mobility differences, we have noted that the various ry^{+} isoalleles are associated with variation in the level of XDH activity, which also behaves as a stable phenotypic character (CHOVNICK *et al.* 1976; CHOVNICK, GELBART and MCCARRON 1977). These are summarized in Table 1, where H refers to high activity, L indicates low activity, and

TABLE 1

Wild type isoalleles of rosy

ry^{+} alleles	Mobility	XDH activity
+12, +13	0.90	N
+14	0.94	N
+10	0.97	L
+0, +6	1.00	N
+1, +11, +16	1.02	N
+4	1.02	H
+2	1.03	N
+3, +5	1.05	N

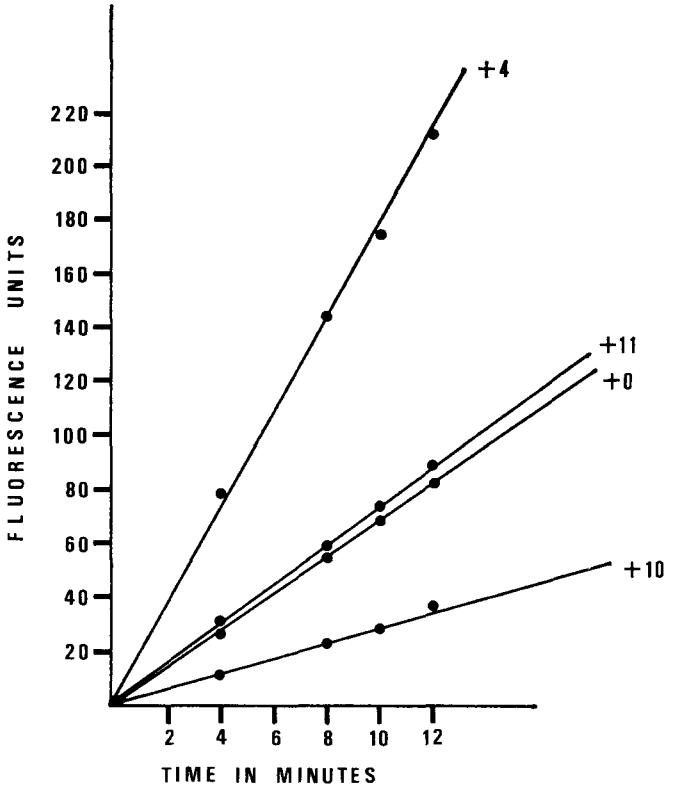

FIGURE 3.—Fluorimetric assay of XDH activities of matched extracts of the indicated homozygous wild-type isoallelic strains.

N refers to a range of intermediate activity levels that we presently classify as normal. Figure 3 illustrates XDH activities of matched preparations of several *ry*+ isoalleles representing the various XDH activity classes presented in Table 1. Measurements of XDH activity/mgm protein, activity/fly or activity/gm wet weight invariably yield similar relationships. Moreover, these activity differences are seen in assays using hypoxanthine (electrophoresis or spectrophotometry) or 2-amino-4-hydroxypteridine (fluorimetry) as substrate.

Genetic analysis of the increased activity over normal associated with ry^{+4} led to the identification of a site, *i409*, responsible for this difference. Thus, the ry^{+4} isoallele possesses *i409H*, while ry^{+0} (and other alleles with normal levels of activity) possesses the *i409N* alternative. Of particular interest is the fact that *i409* is located to the left of the XDH coding element boundary, and to the right of *l(3)S12*, a mutant site in the functionally independent genetic unit immediately to the left of rosy (Figure 4).

Selective system matings: Large-scale genetic fine-structure experiments were carried out making use of the fact that XDH$^-$ or low XDH progeny may be selected against by growth

FIGURE 4.—Map location of *i409* site relative to *l(3)S12* and the XDH structural element.

on purine-supplemented medium. Previous reports described experiments that follow a protocol satisfactory for discriminating between XDH⁻ (or almost XDH⁻) and wild-type levels of activity (CHOVNICK 1973). Since the present report involves intermediate levels of XDH activity, two modified protocols have been used.

Protocol A will kill all XDH⁻ rosy mutant progeny, but will permit the survival of progeny possessing as little activity as does the ry^{+10} strain (Figure 3). Matings involve 40 to 50 females with 20 to 25 males per half-pint milk bottle containing standard Drosophila medium. Following an initial 48 hr egg-laying period, parents are shaken over to fresh food at which time, one ml of 0.11% purine is added to each developing culture. Successive broods involve 24-hr laying periods for up to ten days.

Protocol B will kill all XDH⁻ rosy eye color mutants, and individuals with reduced levels of XDH will also die. While this procedure selects against the survival of individuals with XDH activity levels as high as that of ry^{+10}, occasional "escapers" or survivors of this class are seen. However, the escapers are delayed in development and emerge several days late. Matings involve 70 to 80 females with 20 to 25 females per half-pint milk bottle containing standard medium. Following an initial 24-hr egg-laying period, parents are shaken over onto fresh food, at which time one ml of 0.3% purine is added to each bottle. Successive broods involve 12-hr laying periods for up to ten days.

Enzyme preparation and fluorimetric assay: Unless otherwise indicated, all procedures are carried out at 0° to 5°. Enzyme is prepared as follows: 0.12 gm of flies (eclosing within a six-hr period and incubated overnight on fresh food) are homogenized in 3 ml of 0.1M Tris (hydroxymethyl) aminomethane, pH 8.0, containing 2.7 mg per ml of neutral norit. The homogenate is centrifuged at 25,000 × g for 30 min. One ml of 0.1M Tris, pH 8.0 containing 8.0 mg per ml of neutral norit is added to the decanted supernate, and the mixture centrifuged again at 35,000 × g for another 30 min. The supernate then is filtered through a 0.45μ Type HA Millipore filter, the filtrate serving as enzyme. Fluorimetric assay follows our previous protocol (CHOVNICK *et al.* 1970) except that reaction tubes contain 1.9 ml of 0.1M Tris, pH 8.0, 0.01 ml of 10^{-3}M, 2-amino-4-hydroxypteridine (AHP), 0.02 ml of 10^{-3}M methylene blue and 0.1 ml of enzyme.

Electrophoresis: The electrophoresis procedures are modified from those described previously (MCCARRON, GELBART and CHOVNICK 1974). Principal differences are: The gel consists of 5% acrylamide and 0.25% N,N′-methylenebisacrylamide in a pH 8.9 buffer of 10^{-1}M Tris, 1.7×10^{-3}M disodium ethylenediaminetetraacetate (EDTA) and 4.2×10^{-2}M boric acid, which also serves as the electrophoresis buffer. Electrophoresis is started at 75 ma (~ 250V) and run for five hrs at constant voltage and at 0° to 5°. Gels are developed in an assay mixture containing 1.5×10^{-4}M phenazine methosulfate, 4.0×10^{-4}M ρ-nitroblue tetrazolium, 7.9×10^{-4}M β-diphosphopyridine nucleotide (NAD) and 5.0×10^{-4}M hypoxanthine in a pH 8.5 buffer of 0.1M Tris.

Rocket electrophoresis: This procedure is modified from an earlier description (CHOVNICK *et al.* 1976). After precoating the 3¼ × 4-inch glass slides with unbuffered agarose, a second layer is applied consisting of 14 ml of 1.5% agarose (BioRad 162-0100) buffered in 5.0×10^{-2}M Tris, 5.5×10^{-3}M boric acid and 1.6×10^{-3}M EDTA at pH 8.9 and containing 0.05% anti-XDH serum. Antigen is prepared by grinding 200 adult flies (hemizygotes over a deficiency) or 100 homozygotes in 1.0 ml of 0.1M Tris buffer at pH 8.0, centrifuging and filtering the supernatant. Nine μl samples are placed in 3 mm wells. Plates are run toward the anode for 21 hrs in an EC-660 Immunoelectrophoresis cell (E. C. Apparatus Corp., St. Petersburg, Florida) with a pH 8.9 buffer containing 8.7×10^{-2}M Tris, 2.8×10^{-3}M EDTA and 8.8×10^{-3}M boric acid in the electrode chamber. Plates are developed for XDH activity as described above for electrophoresis.

Enzyme purification: Xanthine dehydrogenase is purified by means of immunoaffinity chromatography (EDWARDS, CANDIDO and CHOVNICK 1977) with the following modifications: Flies are homogenized in 2½ volumes of 0.1M Tris buffer at pH 8.0, containing 4 mM β-mercaptoethanol and 100 μM phenylmethylsulfonyl fluoride (PMSF). After centrifugation at 12,000 × g for 20 min, the supernate is collected, and the pellet homogenized again (as above) and

centrifuged. The supernates are pooled and applied directly to the antibody column. After washing and eluting the column, as described previously, the enzyme is desalted immediately on a Sephadex G-25 column, equilibrated and eluted with 50 mM NH_4HCO_3.

Kinetic measurements were carried out as described previously (EDWARDS, CANDIDO and CHOVNICK 1977).

RESULTS AND DISCUSSION

The present report focuses attention upon the genetic basis for the lower than normal level of XDH activity associated with the ry^{+10} isoallele, which was isolated in 1972 from a single third chromosome recovered from the Bethulie strain. This wild-type strain was obtained from the Drosophila collection of the Department of Zoology, University of Witwatersrand, Johannesburg, South Africa. As noted above (Table 1, Figure 3), it is associated with low XDH activity, and produces an XDH that is slower in electrophoretic mobility (0.97) than the XDH produced by our standard ry^{+0} allele (1.00). Moreover, the ry^{+10} enzyme is somewhat thermolabile relative to the enzyme produced by ry^{+0}.

As a preliminary to subsequent studies, an EMS mutagenesis (LEWIS and BACHER 1968) led to the recovery of several XDH$^-$, rosy eye color mutants (ry^{1001}, ry^{1002} and ry^{1003}).

Genetic fine structure experiments

The first task of the genetic fine-structure study was to determine the approximate location within the rosy region of the genetic basis for the low XDH activity associated with ry^{+10}. To this end, a fine-structure cross testing for recombinants between ry^{1003} and ry^{23} was carried out. The ry^{23} site marks the left boundary of the XDH structural element (Figure 2). In order to permit the survival of ry^+ recombinants that might possess XDH activity levels as low as that of the ry^{+10} parent isoallele, and still select against XDH$^-$ rosy eye color mutants, purine-selection protocol A was used (MATERIALS AND METHODS).

The recombination data are presented in the form used in previous reports (GELBART, MCCARRON and CHOVNICK 1976; CHOVNICK *et al.* 1976). Those recombinants exhibiting exchange for flanking markers are referred to as crossovers, while those exhibiting parental flanking markers are noted as conversions. Each recombinant is tested for electrophoretic mobility, enzyme activity and level of cross-reacting material (CRM) to XDH antibody. Consequently, we classify the ry^+ recombinant allele in brackets indicating mobility and level of XDH activity associated with that allele when examined in heterozygotes carrying a deficiency for the rosy locus. The results of the first experiment are summarized in Table 2, and several points of interest are to be noted:

(1) All of the conversions of ry^{1003} and ry^{23}, in addition to exhibiting the parental flanking markers, are parental types with respect to both electrophoretic mobility and level of XDH activity, confirming the heterozygosity and presence of these genetic characters in the cross. (2) The crossovers locate the allele-complementing mutant site, ry^{1003}, to the right of ry^{23}. (3) Additionally, the crossovers identify a single site, *e1004*, responsible for the mobility difference between the parental isoallele products of ry^{+0} (1.00) and ry^{+10} (0.97). The

TABLE 2

Number and classes of ry+ *chromosomes recovered from progeny of a cross of the indicated females to tester males of the genotype* Dfd Df(3)kar^{31} ry^{60}/kar^{2} Df(3)ry^{75}

Female parent	Crossovers		Conversions, ry^{1003}	Conversions, ry^{23}	Zygotes sampled ($\times 10^6$)
	kar ry+ l(3)26+	*kar+ ry+ l(3)26*	*kar+ ry+ l(3)26+*	*kar ry+ l(3)26*	
+ ry^{1003} + / *kar* ry^{23} *l(3)26*	0	1[1.00L] 1[0.97L]	3[0.97L]	3[1.00N]	0.49

Experiment carried out following Purine Selection Protocol A (MATERIALS AND METHODS).

ry^{+0} allele carries *e1004f* (fast), while ry^{+10} is *e1004s* (slow). Moreover, the crossovers place the electrophoretic site between the ry^{23} and ry^{1003} mutant sites. (4) Finally, the crossovers indicate that the genetic basis for the difference in enzyme activity levels associated with the parental alleles ry^{+10} and ry^{+0} lies to the left of both of the crossover points, and hence lies somewhere on the left side of the rosy region. It should be noted that the crossovers clearly separate the genetic basis for the difference in enzyme activity level from the electrophoretic character.

Are we dealing with a single site? That the genetic basis for the enzyme activity difference is resident in a single site, emerges from the results of the cross summarized in Table 3. In this, and all subsequent fine-structure recombination tests, purine selection protocol B (MATERIALS AND METHODS) was used. This procedure will kill all XDH$^-$ flies, almost XDH$^-$ flies and ry^{+10} flies, but permits wild-type recombinants with normal levels of XDH to survive. Additionally, this procedure permits a low level of "leakage" of ry^{+10} (parental type) survivors in each experiment. While this low level of "noise" in such experiments multiplies the labor involved in analysis of surviving exceptions, there is no problem in their identification. Moreover, this "leakage" ensures that should recombination produce alleles associated with XDH activity levels intermediate to ry^{+10} and ry^{+0}, they would be recovered and scored in our experiments.

Table 3 summarizes the results of an experiment testing for recombination between the genetic basis for low XDH activity of the ry^{+10} allele and the ry^{8} site (an XDH$^-$, rosy eye color mutant of the ry^{+0} allele). Note that the brackets

TABLE 3

Number and classes of ry+ *chromosomes recovered from progeny of a cross of the indicated females to tester males of the genotype* Dfd Df(3)kar^{31} ry^{60}/kar^{2} Df(3)ry^{75}

Female parent	Crossovers	Conversions, ry^{+10}	Conversions, ry^{8}	Zygotes sampled ($\times 10^6$)
	kar ry+ l(3)26+	*kar+ ry+ l(3)26+*	*kar ry+ l(3)26*	
+ ry^{+10} [+ *e1004s*] + / *kar* ry^{8} [*8 e1004f*] *l(3)26*	6[0.97N]	10[0.97N]	6[1.00N] 4[0.97N]	1.17

Experiment carried out following Purine Selection Protocol B (MATERIALS AND METHODS).

around the known heterozygous rosy locus sites in the female parent genotype indicate ambiguity in relative position. The following features of the data of Table 3 are to be noted: (1) The genetic basis for the difference in XDH activity associated with ry^{+10} and the ry^{+0} allele (Table 1) lies to the left of all crossover points and clearly separates level of activity from both the ry^{8} site and the *e1004* site. (2) There were no recombinants associated with intermediate levels of XDH activity among either the crossovers or the conversion classes of this or any other experiment. This fact permits us to identify a single site responsible for the difference in level of XDH activity, *i1005*. We refer to ry^{+10} as *i1005L* (Low), while ry^{+0} possesses the *i1005N* alternative. Thus, the ten conversions of ry^{+10} recovered in this experiment (Table 3) are conversions, *i1005L* → *i1005N*. (3) On the basis of relative frequency of co-conversion with the ry^{8} site (40%), we localize *e1004* to the vicinity of ry^{8}.

Location of i1005 *relative to the structural element boundary*: Thus far, experiments have been described that associate the difference in level of XDH activity seen between ry^{+10} and the normal activity associated with ry^{+0} to a single site, *i1005*, located somewhere on the left side of the rosy locus. Table 4 summarizes the results of an experiment designed to locate this site relative to the left boundary of the XDH coding element as marked by the mutant site, ry^{23}. Major features of these data are: (1) *i1005* is located well to the left of ry^{23}, and hence to the left of the XDH structural element boundary. (2) The failure to recover intermediates in level of XDH activity among the recombinants provides additional evidence in support of the conclusion drawn in the previous section that we are dealing with a single site. (3) Conversions of ry^{23} include some co-conversions of the electrophoretic site (25%).

Are i1005 *and* i409 *separable sites?* At this juncture, one is drawn to the possibility that the observed variation in level of XDH activity (Low, Normal and High) characterizing our various ry^{+} alleles (Table 1) may reflect alternatives that map to the same site. Might *i1005* and *i409* be synonyms designating the same site, or do they mark separable sites? Table 5 summarizes the results of a cross designed to answer this question. Essentially, heterozygotes of the genotype + *L* + / *kar H* ry^{406} were mated to appropriate tester males following a selective

TABLE 4

Number and classes of ry+ *chromosomes recovered from progeny of a cross of the indicated females to tester males of the genotype* Dfd Df(3)kar^{31} ry^{60}/kar^{2} Df(3)ry^{75}

Female parent	Crossovers	Conversions, $ry^{+i1005L}$	Conversions, ry^{23}	Zygotes sampled ($\times 10^6$)
	kar ry+ l(3)26+	*kar+ ry+ l(3)26+*	*kar ry+ l(3)26*	
+ *i1005L* + *e1004s* + / *kar i1005N 23 e1004f l(3)26*	6[0.97N]	5[0.97N]*	6[1.00N] 2[0.97N]	1.20

Experiment carried out following Purine Selection Protocol B (MATERIALS AND METHODS).

* This class may be under-represented. This phenotypic class (*kar+ ry+ l(3)26+*) includes the "leaking" parental class among later eclosing exceptions. Since early eclosing exceptions revealed the crossovers to be among the phenotypically *kar* progeny, analysis of exceptions was then restricted to *kar* progeny in order to collect crossover frequency data for mapping.

TABLE 5

Number and classes of ry+ *chromosomes recovered from progeny of a cross of the indicated females to tester males of the genotype* Df(3)ry^{36}/Tp(3)MKRS, M(3)S34 kar ry^{2} Sb

Female parent	Crossovers *kar ry+ pic+ l(3)26*	Conversions, ry^{i1005L} *kar+ ry+ pic+ l(3)26*	Conversions, ry^{406} *kar ry+ pic^{G23i} l(3)26+*	Zygotes sampled (× 10^{6})
+ *i1005L* + *e1004s e408s* + *l(3)26*	9[0.97H]	1[0.97N]	3[1.02H]	1.3
kar^{2} i409H 406 e1004f e408f pic^{G23i} +	3[0.97N]			

Experiment carried out following Purine Selection Protocol B (MATERIALS AND METHODS).

protocol designed to kill *L* and ry^{406} bearing progeny. The additional markers in the cross (Table 5) provide additional control in the experiment.

If *i1005L* and *i409H* are located at the same site, then all crossovers should exhibit the high activity associated with *i409H*. Similarly, conversions of *i1005L* should yield *i409H*. In fact, neither of these expectations are fulfilled. Rather, the one conversion of *i1005L* yields normal activity, and the crossovers fall into two classes, High and Normal. These data indicate quite definitely that *i1005* and *i409* mark separable sites.

Unfortunately, this experiment is unable to determine the relative positions of the two sites because we do not know what effect the double variant, *i1005L i409H*, might have on XDH activity. Figure 5 illustrates the ambiguity in our present situation. If the double variant is associated with less than normal levels of XDH activity, then the map order illustrated in Figure 5A is correct. In this case, *i1005* is located to the left of *i409*, and thus still further from the left border of the XDH coding element. On this model, the 12 recovered crossovers involve exchange at the indicated positions. Crossover class (1) represents the nine high XDH activity crossovers, while class (2) describes the three normal XDH ac-

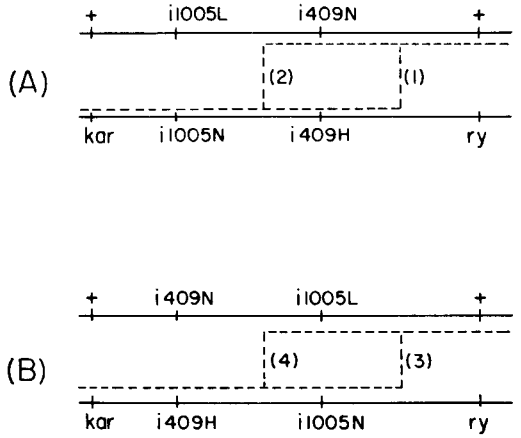

FIGURE 5.—Alternative map positions of *i1005* and *i409*. Ambiguity inherent in random strand mapping experiment.

tivity crossovers. On the other hand, if the double variant, *i1005L i409H*, is associated with normal activity, then the possibility remains that the reverse order illustrated in Figure 5B might be correct. Resolution of this ambiguity requires further experiments, which are in progress, and will be reported separately.

Location of i1005 *relative to* l(3)S12: Having positioned the *i1005* site to the left of the XDH coding element boundary, and separable from *i409*, we should next consider its position relative to the left boundary of the putative XDH control element. This boundary presently is marked by *l(3)S12*, a mutant site in the genetic unit immediately to the left of rosy (Figure 4). In view of the proximity of *i1005* to the left boundary of the XDH structural element (Table 4) and to *i409* (Table 5), it is reasonable to assume that *i1005* is located to the right of *l(3)S12*, and hence within the region designated as the XDH control element. Confirmation of this notion is seen in the data presented in Table 6. Matings of the indicated parents were carried out following purine protocol B, which selects against *i1005L* with some leakage. Additionally, *l(3)S12* dies with *Df(3)ry*^{75}, and *l(3)26* dies as a homozygote, but survives with *Df(3)ry*^{75}. Anticipating a very low frequency of single crossovers between *l(3)S12* and *i1005*, the experiment was carried out in two very large-scale crosses to yield a total estimated sample of 5.0×10^6 progeny. Diagnosis of survivors was restricted to the *kar*+ progeny, which totaled 731. In addition to "leakers," which are nonrecombinant + + *i1005L e1004s* + parental types, this cross produced an array of triploids, aneuploids and possibly unequal crossovers. The last class may have been among a group of sterile *kar*+ survivors that could not be further tested. However, complete analysis of the viable, fertile *kar*+ survivors yielded 55 recombinants indicated in Table 6. There were no diagnosed unequal crossovers carrying duplications for the rosy region among the viable and fertile survivors.

Analysis of the diagnosed *kar*+ chromosomes recovered from survivors of the cross of Table 6 is most easily understood on the hypothesis that *i1005* is located to the right of *l(3)S12*. Class (a) represents single crossovers between *l(3)S12*

TABLE 6

Number and classes of kar+ ry+ *recombinant chromosomes recovered from progeny of the indicated cross*

Female parent							Male parent		
+	+		*i1005L*	*e1004s*	+		*kar*^{2}	*Df(3)ry*^{75}	
kar^2	*l(3)S12*		*i1005N*	*e1004f*	*l(3)26*	×	*kar*^{2}	*ry*^{8}	*l(3)26*

↓ Purine Protocol B

(a) (7) *kar*+ *l(3)S12*+ *i1005N e1004f l(3)26* [1.00N]
(b) (44) *kar*+ *l(3)S12*+ *i1005N e1004s l(3)26*+ [0.97N]
(c) (3) *kar*+ *l(3)S12* *i1005N e1004s l(3)26*+ [0.97N]
(d) (1) *kar*+ *l(3)S12*+ *i1005N e1004f l(3)26*+ [1.00N]

Zygotes sampled = 5.0×10^6

and *i1005*. Class (b) represents conversions of *i1005L* → *i1005N*, while class (c) are conversions of *i1005L* that also are co-conversions *l(3)S12*$^+$ → *l(3)S12*. Since one-half of the *l(3)S12* progeny die, we assume that the frequency of co-conversion is twice that observed. Finally, the single member of class (d) is most simply understood as a crossover between *l(3)S12* and *i1005* accompanied by a second event (most likely a conversion, *l(3)26* → *l(3)26*$^+$). The frequency of conversion of *i1005L*, $50/5 \times 10^6$, is entirely consistent with that observed previously (Table 3), and the estimated map distance between *l(3)S12* and *i1005* is $15 \times 2 \times 10^2/5 \times 10^6 = 6 \times 10^{-4}$ map units.

Biochemical Studies

In a previous report (CHOVNICK *et al.* 1976), we provided evidence for the existence of a *cis*-acting control element adjacent to the XDH structural information. We argued that this region consists of one or more DNA sequences that serve to regulate rosy locus function rather than to code for part of the XDH peptide. Hence, one should expect that variants mapping in this region would be associated with phenotypes reflecting a regulatory alteration. A corollary would argue that such variation not be associated with a change in the structure of the XDH peptide. The following experiments examine these questions with respect to variation at the *i1005* site.

Thermolability studies: As noted above and illustrated in Figure 6, the ry^{+10} enzyme is thermolabile relative to that produced by ry^{+0} (and other standard ry^+ isoalleles as well). Might the thermolability of the ry^{+10} enzyme reflect an *XDH* structural alteration brought about by *i1005L*? On this hypothesis, the thermolability might reflect a more general molecular instability resulting in decreased numbers of XDH molecules per fly and hence the decreased XDH activity associated with ry^{+10}. That this is not the case can be seen from the thermal inactivation experiment described in Figure 6. Here, matched extracts of several genotypes are compared for XDH activity following 48° heat inactivation over a time range from zero to ten minutes. The thermolability difference between ry^{+10} and ry^{+0} is clearly illustrated. A third extract examined, ry^{+r} (1.00L), was obtained from a crossover resulting from an experiment discussed above, and described in Table 2. Essentially, *i1005L* + *e1004s 1003/i1005N 23 e1004f* + ♀♀ were crossed to appropriate tester males on purine supplemented medium, and two ry^+ crossovers were recovered among the recombinants. Both exchange points were located to the right of ry^{23}. One was located between ry^{23} and the electrophoretic site, *e1004*, thus producing a ry^+ recombinant allele carrying *i1005L* + *e1004f* +. The XDH phenotype associated with this allele exhibits the mobility of ry^{+0} (1.00) and the low activity associated with the *i1005L* site of ry^{+10}. As noted earlier, this result clearly separates the level of activity phenotype from the electrophoretic character. Moreover, examination of the thermolability of this recombinant (Figure 6) reveals that it is identical to that of the ry^{+0} product, rather than to that of the ry^{+10} enzyme. In addition to separating *i1005L* from the thermolability associated with ry^{+10}, this observation places the genetic basis for the ry^{+10} thermolability to the right of the crossover point, and hence, clearly locates it within the structural element.

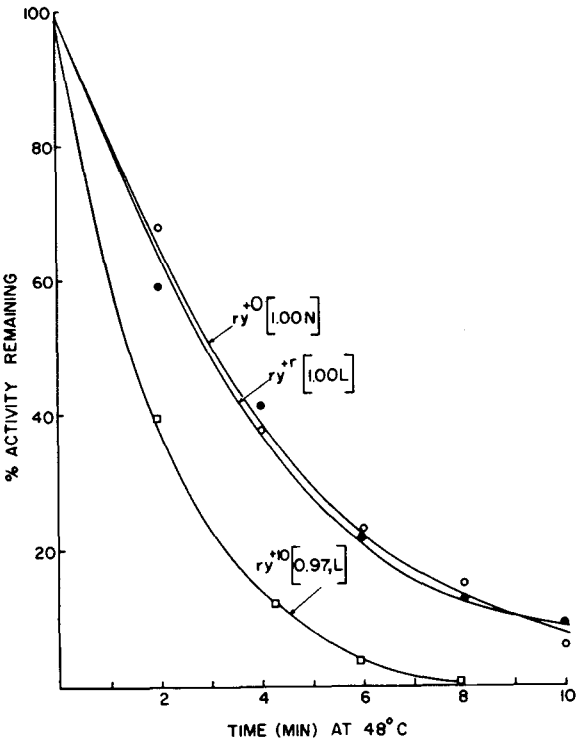

FIGURE 6.—Heat inactivation of XDH in matched extracts of the following strains:
ry+0 = cu kar ry+0 (i1005N, e1004f) l(3)26/TP(3)MKRS, M(3)S34 kar ry2 Sb.
ry+r = ry+r (i1005L, e1004f) l(3)26/TP(3)MKRS, M(3)S34 kar ry2 Sb.
ry+10 = ry+10 (i1005L, e1004s) l(3)26/TP(3)MKRS, M(3)S34 kar ry2 Sb.

Kinetic studies: We may next consider the possibility that differences in level of XDH activity between ry^{+10} and other ry^{+} isoalleles may be due to XDH structural differences that affect kinetic parameters of the purified enzyme. Previous studies (EDWARDS, CANDIDO and CHOVNICK 1977), which compared the purified enzymes from ry^{+4} and ry^{+11}, demonstrated: (1) That the enzyme reaction in both cases followed a "ping-pong" mechanism similar to that seen with avian XDHs and milk xanthine oxidase. (2) The K_m values for substrate and NAD^+ at infinite substrate and NAD^+ concentrations were not significantly different for the enzymes from ry^{+4} and ry^{+11}. Following the same procedures, pure XDH from ry^{+10} and ry^{+0} were compared. In addition to observing the "ping-pong" reaction kinetics, the K_m values for the ry^{+10} and ry^{+0} enzymes did not differ significantly from each other, nor did they differ from the ry^{+4} and ry^{+11} data collected earlier (Table 7). Consequently, we reject the notion that differences in XDH activity of the magnitude seen in these strain comparisons (Figure 3) might be attributed to XDH structural differences that effect alterations in enzyme affinity for substrate or NAD^+.

TABLE 7

K_m *values for pure XDH isolated from homozygotes for the indicated* ry+ *isoalleles*

Substrate	K_m, moles/liter × 10^5			
	ry^{+10}	*ry*$^{+0}$	*ry*$^{+11*}$	*ry*$^{+4*}$
Xanthine	2.0	1.6	2.4	2.1
NAD+	3.5	3.7	4.0	2.6

Values were determined from best fit lines by linear regression analysis.
* From EDWARDS, CANDIDO and CHOVNICK 1977.

Immunological experiments support the view that the differences in XDH activity levels associated with the various *ry*+ isoalleles (Figure 3) reflect differences in number of XDH molecules. Figure 7 presents a typical immunoelectrophoresis experiment utilizing the method of "rocket electrophoresis" (LAUREL 1966; WEEKE 1973) to compare the relative numbers of molecules of XDH in matched extracts of *ry*$^{+11}$, *ry*$^{+10}$, *ry*$^{+0}$ and *ry*$^{+4}$ homozygotes. The XDH antibody preparation is the same as that described in a prior report (CHOVNICK *et al.* 1976). Quantitative analysis of such gels (CHOVNICK *et al.* 1976) reveals that the rocket heights parallel quite closely the XDH activity levels associated with these isoalleles.

Relationship between i409, i1005 *and the XDH structural element*

Might i1005L *mark a tandem duplication of the XDH structural element?* In prior reports, we have considered and eliminated the possibility that *i409H* might mark a tandem duplication of the XDH structural element (CHOVNICK *et al.* 1976; CHOVNICK, GELBART and MCCARRON 1977). While the association of *i1005L* with a reduction in the number of XDH molecules per fly does not immediately suggest a tandem duplication, the Bar duplication in *Drosophila melanogaster* and its associated position effect (STURTEVANT 1925; MULLER *et al.* 1936; BRIDGES 1936; MULLER 1936) provides ample precedence for such

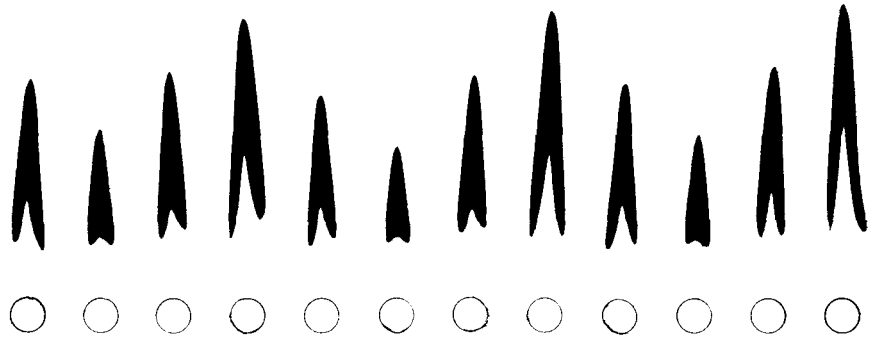

FIGURE 7.—"Rocket" electropherogram. Matched extracts of homozygotes run against anti-XDH serum. From left to right, *ry*$^{+11}$, *ry*$^{+10}$, *ry*$^{+0}$ and *ry*$^{+4}$ repeated in that order across the gel.

a model. On this notion, the ry^{+10} isoallele would possess two XDH structural elements in tandem. By virtue of the change in position of each member of the duplex relative to some adjacent genetic element(s), a disturbed function of both XDH structural elements, results. Such a model is precluded on several counts:

(1) The ry^{+10} allele is associated with a single XDH electrophoretic band of the mobility class, $XDH^{0.97}$ (Table 1). XDH is a homodimer, and the presence of two electrophoretically distinct structural elements will produce individuals possessing three XDH moieties. The tandem duplication model then requires that the ry^{+10} allele possess two XDH structural elements whose peptide products are indistinguishable, and of the mobility class, $XDH^{0.97}$. Thus, *1005L* should be associated with an $XDH^{0.97}$. On this point, the tandem duplication model fails. In the course of various experiments, we have recovered recombinant isoalleles which place *i1005L* with structural elements producing $XDH^{1.00}$ and $XDH^{1.05}$ molecules. While both recombinant alleles are associated with the low level of XDH activity characteristic of *i1005L*, there is no indication of the production of an $XDH^{0.97}$ dimer or even of a hybrid dimer.

(2) Tandem duplications are characterized by instability in homozygotes due to increased incidence of unequal exchange events. The ry^{+10} stock has been quite stable.

(3) EMS mutagenesis of ry^{+10} has produced XDH^- rosy eye color mutants at a frequency that does not distinguish this allele from other ry^+ isoalleles.

(4) Cytological examination of polytene chromosomes of ry^{+10} bearing strains reveals no evidence of tandem duplication.

Might i1005, *and* i409 *as well, mark sites within the XDH control element?* As noted above, the rosy locus genetic maps of Figure 2 establish the genetic boundaries of the XDH coding element. As a result of extensive mapping experiments over a number of years, these boundaries enclose a region that today includes 60 sites representing all of the mapped XDH^- rosy eye color mutant sites, sites of electrophoretic variation and "leaky" structural mutant sites. Eventually, we hope to relate these genetic boundaries to the amino and carboxy termini of the XDH peptide. However, the fact that these boundaries have not changed in recent years (GELBART *et al.* 1974; GELBART, MCCARRON and CHOVNICK 1976), coupled with the extensive data upon which they are based, strongly suggests that the present genetic boundaries may well approximate the amino and carboxy termini.

Only two mapped sites fall outside of the coding element boundaries. Both mark sites (*i1005* and *i409*) whose variants are associated with phenotypic effects that conform precisely with expectation for control element variants.

In a previous report (CHOVNICK *et al* 1976), evidence was presented that demonstrated the *cis*-acting nature of *i409* variation. Figure 8 presents an electropherogram demonstrating that the *cis*-acting nature of *i409* variation may be extended to *i1005* as well. The photograph is printed as a negative in order to enhance the contrast between XDH bands and the acrylamide slab gel. Allele designations are presented in Figure 8 in terms of electrophoretic mobility and

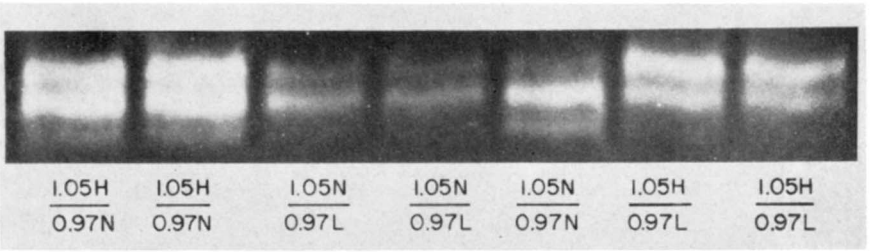

FIGURE 8.—XDH electropherogram indicating the relative amounts of $XDH^{1.05}$, $XDH^{1.01}$ and $XDH^{0.97}$ present in matched extracts of flies heterozygous for the indicated combinations of structural and control elements.

level of XDH activity. Thus, *1.05H* refers to a recombinant ry^+ allele exhibiting the fast mobility of the ry^{+5} allele (Table 1), and the high XDH activity level of the ry^{+4} allele. In terms of intensity sites, this allele should be considered as *i1005N, i409H*. Those alleles with activity levels designated as N are *i1005N, i409N* while L refers to *i1005L, i409N*. The heterozygote marked $\frac{1.05N}{0.97N}$ illustrates the characteristic 1:2:1 three-banded pattern of XDH dimers to be found in a heterozygote possessing approximately equal proportions of the fast and slow monomers. Intensity site substitutions ,as indicated in Figure 8, produce heterozygotes whose XDH electrophoretic gel patterns indicate that the *i1005* and *i409* sites are *cis*-acting at the level of XDH monomers, to determine the number of monomers available for dimer formation.

On the basis of these observations, we are drawn to the possibility that *i1005* and *i409* mark the 5′ control element of the rosy locus. Although the present state of this analysis is reminiscent of early stages in the analysis of the *lac* region promoter in *E. coli* (IPPEN *et al.* 1968; ARDITTI, SCAIFE and BECKWITH 1968), we caution the reader that the present data do not, as yet, permit specification of the control function involved in either *i409* or *i1005* variation. Certainly, it is reasonable to expect that *cis*-acting variants of the 5′ control element might involve alterations in DNA sequences that serve as binding sites for regulatory signal(s), sites for RNA polymerase binding and initiation of transcription, transcript processing sites, ribosome binding and initiation of translation. In view of the significant recombination between *i1005* and *i409*, it is quite possible that these sites mark different DNA sequences in the control element, and thus involve variation in different control functions.

Structural and control element size estimates: Figure 9 summarizes our present "best" estimates of map lengths for the rosy locus structural and control elements. Boundaries for the structural element are described in an earlier section. The XDH structural element map distance of 5×10^{-3} map units emerges from an enormous data base (Figure 2), and is not likely to change. However, control element mapping data is limited, and size estimates should be considered as quite tentative. Indeed, the present estimate (Figure 9), which we believe to be considerably better than our past effort (CHOVNICK *et al.* 1976; CHOVNICK

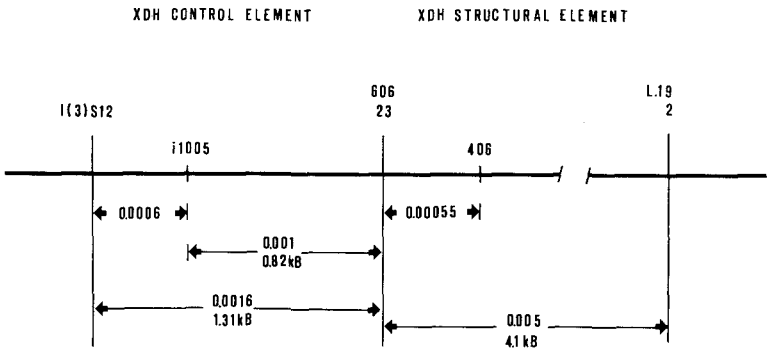

FIGURE 9.—The rosy locus. Size estimates of the structural and control elements.

et al. 1977), represents a significant downward revision of the size of the control element. The distance from *i1005* to ry^{23} and the structural element left border emerges from the data of Table 4, while the distance from *l(3)S12* to *i1005* is estimated from the experiment summarized in Table 6. These emerge from recombination experiments that sampled 1.2×10^6 and 5.0×10^6 progeny, respectively. Independent support of this map is seen as follows: the estimated map distance of the structural mutant site, ry^{406}, from the left border of the structural element is obtained from the average of two large recombination experiments (tests against ry^{606} and ry^{23}) with similar results (GELBART, MCCARRON and CHOVNICK 1976) involving a sample of 2.2×10^6 progeny. Thus, the summed distances of (*i1005* to ry^{23}) + (ry^{23}, ry^{606} to ry^{406}) $= 1.55 \times 10^{-3}$ map units. Consider now the results of the experiment summarized in Table 5 demonstrating that *i1005* and *i409* are genetically separable sites. Although this experiment failed to provide the relative order of the two sites (Figure 5), estimates of the map distance of these sites from ry^{406} may be drawn (1.38×10^{-3} and 1.84×10^{-3} map units, respectively). Both estimates are strikingly close to the summed estimate described above.

How, then, do we reconcile the present map (Figure 9) with the much larger estimate of the control element size presented earlier (CHOVNICK *et al.* 1976; CHOVNICK *et al.* 1977)? The latter derived from the pooled results of two recombination experiments with quite disparate results. Those experiments provided mapping data for the region *l(3)S12–i409–*ry^{402} and *l(3)S12–i409–*ry^{406}. The ry^{402} and ry^{406} sites are both located within the leftmost one-tenth of the structural element (which might best be estimated by the distance given for ry^{406} in Figure 9). Now, let us consider the map estimates from these data (CHOVNICK *et al.* 1976) taken separately, and compare them with our present estimates. The mapping data involving the ry^{402} site sampled 0.82×10^6 progeny and estimated the distance *l(3)S12* to *i409* $= 0.98 \times 10^{-3}$, and *i409* to $ry^{402} = 1.46 \times 10^{-3}$ map units, respectively. These data are quite consistent with our present estimates. The other experiment was a small sampling (0.36×10^6 progeny), which yielded quite aberrant estimates for *l(3)S12* to *i409* $= 4.4 \times 10^{-3}$ and *i409* to $ry^{406} = 12.2 \times 10^{-3}$ map units, respectively. Given the large variance associated

with such a Poisson variate where each rare crossover event is multiplied by a factor of four, as well as the small sample involved in this deviant result, we feel quite justified in setting aside this single result in composing our present map (Figure 9).

Translation of map distance estimates into DNA base lengths proceeds from the XDH peptide molecular weight of 150,000 daltons. Assuming an average amino acid molecular weight (adjusted for peptide linkage) to be 110, then the number of nucleotides in the structural element required to code for such a peptide is approximately 4.1 kB (150,000 × 3/110). Then, from the recombination map length of the structural element (0.005 map units), we relate map length to number of bases (0.01 map unit = 8.2 kB), which we apply directly to the adjacent control element (Figure 9).

Although the present data demand a downward revision of the control element size estimated previously, there is no reason to consider revision of our designation of *i409* as a control element site. The biochemical analysis coupled with the crossover data (CHOVNICK *et al.* 1976) and co-conversion data (CHOVNICK *et al.* 1977) provide a compelling argument for its location and designation. There is even a consistency in map distance between the present data and the one large-sized experiment reported previously (see previous section). Thus, in the recombination experiment that mapped *l(3)S12–i409–ry*^{402}, the *i409* site is placed 0.98×10^{-3} map units to the right of *l(3)S12* and 1.46×10^{-3} map units to the left of *ry*^{402}. This location within the control element of Figure 9 is entirely reasonable in view of the data of Table 5 discussed earlier. Considering the total available recombination data, the most reasonable relative position of *i409* would place it closer to the structural element border than *i1005*. However, unambiguous resolution of this issue awaits the results of additional experiments.

It should be appreciated that the extrapolation from recombination map distance to DNA base length assumes that the XDH structural element is not interrupted by one or more nontranslated insert regions. The present, wholly genetic, analysis is unable to provide evidence one way or another on this point. If such an insert were present in the structural element DNA, and if it were to participate in recombination, then we would have underestimated the relationship of nucleotide bases to map distance, and consequently have underestimated the size of the XDH control element as well (Figure 9).

We wish to acknowledge the skillful technical assistance of FLORENCE W. JOHNSTON and LAURA YEDVOBNICK.

LITERATURE CITED

ARDITTI, R. R., J. G. SCAIFE and J. R. BECKWITH, 1968 The nature of mutants in the lac promoter region. J. Mol. Biol. **38:** 421–426.

BLAKE, C. C. F., 1978 Do genes-in-pieces imply proteins-in-pieces? Nature **273:** 267.

BRACK, C. and S. TONEGAWA, 1977 Variable and constant parts of the immunoglobulin light chain gene of a mouse myeloma cell are 1250 nontranslated bases apart. Proc. Natl. Acad. Sci. U.S. **74:** 5652–5656.

BREATHNACH, R., J. L. MANDEL and P. CHAMBON, 1977 Ovalbumin gene is split in chicken DNA. Nature **270**: 314–319.

BRIDGES, C. B., 1936 The Bar "Gene" a duplication. Science **83**: 210–211.

CHOVNICK, A., 1973 Gene conversion and transfer of genetic information within the inverted region of inversion heterozygotes. Genetics **75**: 123–131.

CHOVNICK, A., G. H. BALLANTYNE, D. L. BAILLIE and D. G. HOLM, 1970 Gene conversion in higher organisms: Half-tetrad analysis of recombination within the rosy cistron of *Drosophila melanogaster*. Genetics **66**: 315–329.

CHOVNICK, A., W. GELBART and M. MCCARRON, 1977 Organization of the rosy locus in *Drosophila melanogaster*. Cell **11**: 1–10.

CHOVNICK, A., W. GELBART, M. MCCARRON, B. OSMOND, E. P. M. CANDIDO and D. L. BAILLIE, 1976 Organization of the rosy locus in *Drosophila melanogaster*: Evidence for a control element adjacent to the xanthine dehydrogenase structural element. Genetics **84**: 233–255.

CHOVNICK, A., M. MCCARRON, A. HILLIKER, J. O'DONNELL, W. GELBART and S. CLARK, 1977 Gene organization in Drosophila. Cold Spring Harbor Symp. Quant. Biol. **42**: 1011–1021.

DOOLITTLE, W. F., 1978 Genes in pieces: were they ever together? Nature **272**: 581–582.

EDWARDS, T. C. R., E. P. M. CANDIDO and A. CHOVNICK, 1977 Xanthine dehydrogenase from *Drosophila melanogaster*. A comparison of the kinetic parameters of the pure enzyme from two wild-type isoalleles differing at a putative regulatory site. Molec. Gen. Genet. **154**: 1–6.

GELBART, W., M. MCCARRON and A. CHOVNICK, 1976. Extension of the limits of the XDH structural element in *Drosophila melanogaster*. Genetics **84**: 211–232.

GELBART, W. M., M. MCCARRON, J. PANDEY and A. CHOVNICK, 1974 Genetic limits of the xanthine dehydrogenase structural element within the rosy locus in *Drosophila melanogaster*. Genetics **78**: 869–886.

GILBERT, W., 1978 Why genes in pieces? Nature **271**: 501.

GLOVER, D. M. and D. S. HOGNESS, 1977 A novel arrangement of the 18S and 28S sequences in a repeating unit of *Drosophila melanogaster* rDNA. Cell **10**: 167–176.

IPPEN, K., J. H. MILLER, J. G. SCAIFE and J. R. BECKWITH, 1968 New controlling element in the *lac* operon of *E. coli*. Nature **217**: 825–827.

JEFFREYS, A. J. and R. A. FLAVELL, 1977 The rabbit β-globin gene contains a large insert in the coding sequence. Cell **12**: 1097–1108.

LAI, E. C., S. L. C. WOO, A. DUGAICZYK, J. F. CATTERALL and B. W. O'MALLEY, 1978 The ovalbumin gene: Structural sequences in native chicken DNA are not contiguous. Proc. Natl. Acad. Sci. U.S. **75**: 2205–2209.

LAURELL, C.-B., 1966 Quantitative estimation of proteins by electrophoresis in agarose gel containing antibodies. Anal. Biochem. **15**: 45–52.

LEWIS, E. B. and F. BACHER, 1968 Method for feeding ethyl methanesulfonate (EMS) to Drosophila males. Drosophila Inform. Serv. **43**: 193.

LINDSLEY, D. L. and E. H. GRELL, 1968 *Genetic variations of* Drosophila melanogaster. Carnegie Inst. Wash. Publ. No. **627**.

MCCARRON, M., W. GELBART and A. CHOVNICK, 1974 Intracistronic mapping of electrophoretic sites in *Drosophila melanogaster*: Fidelity of information transfer by gene conversion. Genetics **76**: 289–299.

MCREYNOLDS, L., B. W. O'MALLEY, A. D. NISBET, J. E. FOTHERGILL, D. GIVOL, S. FIELDS, M. ROBERTSON and G. G. BROWNLEE, 1978 Sequence of chicken ovalbumin mRNA. Nature **273**: 723–728.

MULLER, H. J., 1936 Bar duplication. Science **83**: 528–530.

MULLER, H. J., A. A. PROKOFYEVA-BELGOVSKAYA and K. V. KOSSIKOV, 1936 Unequal crossing-over in the Bar mutant as a result of duplication of a minute chromosome section. C. R. (Dokl.) Acad. Sci. U.S.S.R., N.S., **1** (10): 87–88.

PELLEGRINI, M., J. MANNING and N. DAVIDSON, 1977 Sequence arrangement of the rDNA of *Drosophila melanogaster*. Cell **10**: 213–224.

STURTEVANT, A. H., 1925 The effects of unequal crossing-over at the Bar locus in Drosophila. Genetics **10**: 117–147.

TILGHMAN, S. M., J. J. CURTIS, D. C. TIEMEIER, P. LEDER and C. WEISSMAN, 1978a The intervening sequence of a mouse β-globin gene is transcribed within the 15S β-globin mRNA precursor. Proc. Natl. Acad. Sci. U.S. **75**: 1309–1313.

TILGHMAN, S. M., D. C. TIEMEIER, J. G. SEIDMAN, B. M. PETERLIN, M. SULLIVAN, J. V. MAIZEL and P. LEDER, 1978b Intervening sequence of DNA identified in the structural portion of a mouse β-globin gene. Proc. Natl. Acad. Sci. U.S. **75**: 725–729.

WEEKE, B., 1973 Rocket immunoelectrophoresis. In: *A Manual of Quantitive Immunoelectrophoresis: Methods and Applications*. Edited by N. H. AXELSON, J. KROLL and B. WEEKE. Scand. J. Immunol. **2** Suppl. 1: 37–46.

WEINSTOCK, R., R. SWEET, M. WEISS, H. CEDAR and R. AXEL, 1978 Intragenic DNA spacers interrupt the ovalbumin gene. Proc. Natl. Acad. Sci. U.S. **75**: 1299–1303.

WELLAUER, P. K. and I. B. DAWID, 1977 The structural organization of ribosomal DNA in *Drosophila melanogaster*. Cell **10**: 193–212.

WHITE, R. L. and D. S. HOGNESS, 1977 R loop mapping of the 18S and 28S sequences in the long and short repeating units of *Drosophila melanogaster* rDNA. Cell **10**: 177–192.

Corresponding editor: L. SANDLER